Journal of Materials Chemistry B

Accepted Manuscript

ROYAL SOCIETY OF CHEMISTRY

www.rsc.org/materialsB

Journal Name

ARTICLE

Inverse high internal phase emulsion polymerization (i-HIPE) of GMMA, HEMA and GDMA for preparation of superporous hydrogels as tissue engineering scaffold.

Archana C. Nalawade[a], R. V. Ghorpade[c], Sadiqua Shadbar[d], Mohammed Shadbar Qureshi*[a,b], N.N. Chavan[c], Ayesha A. Khan[e] and S. Ponrathnam[c].

Received 00th January 20xx,
Accepted 00th January 20xx

DOI: 10.1039/x0xx00000x

www.rsc.org/

A series of novel superporous hydrogels for regenerative medicine were prepared by oil-in-water (o/w) or inverse high internal phase emulsion (i-HIPE) copolymerization of glycerol monomethacrylate (GMMA), 2-hydroxy ethyl methacrylate (HEMA) and glycerol dimethacrylate (GDMA) as cross-linker using a non toxic solvent and a redox initiator system at the physiological temperature (37 °C). The monomer GMMA was synthesized from glycidyl methacrylate (GMA) by alternative facile method using Amberlyst-15. The described i-HIPEs had shown significantly wider stability window. The polyHIPE hydrogels were characterized by FTIR, BET method for surface area, mercury porosimetry, SEM, DSC, TGA, XRD, compressive strain and strain recovery. The swelling ratio of the hydrogels and their degradation in 0.007 M NaOH and lipase B (*Candida antarctica*) solutions were determined gravimetrically and the rate of degradation was explained in terms of molecular structure of the hydrogels. The morphological studies showed that the pore diameter varied between 20-30 µm and the pore throats (interconnecting windows) diameter in the range of 4-8 µm. The described polyHIPE hydrogels were found to have open cell morphology and interconnected pore architecture – the important characteristics for scaffold applications. The initial cytotoxicity study performed according to ISO-10993-5 indicated cytocompatibility (97% cell viability) and the subsequent cell seeding and proliferation study exhibited 55 - 88 % cell viability (increased monotonously from GHG-1 to GHG-5), which could be attributed to modulation of the physical and chemical properties of the hydrogels. The described super porous hydrogels are considered as potential candidate for scaffold materials in tissue engineering applications.

Introduction

The emerging field of tissue engineering attempts to repair damaged tissues with the help of porous scaffold materials having the required properties which act as a template for tissue regeneration.[1] Polymer based porous materials, as scaffolds, have attracted the attention of researchers due to their versatile properties and applications in this field.[2] The material to be used as a scaffold should permit cells adhesion and promote their growth, and allow the retention of differentiated cell functions besides being biocompatible.[3,4] The micro structural parameters such as porosity, pore size, pore interconnectivity influence the cell attachment, cell growth and their proliferation.[5] Therefore, a scaffold should have high enough porosity to provide sufficient space for cell adhesion, extracellular matrix regeneration and it must allow spatial cell distribution throughout the scaffold to facilitate homogeneous tissue formation.[6-9]

Hydrogels are three dimensional physically or chemically cross-linked polymer networks that can absorb and retain large amounts of water or physiological fluids while maintaining the structural integrity.[10, 11] The porous hydrogels are promising materials as scaffolds for tissue engineering because of their inherent hydrophilic nature; favorable mass transport properties [12-14] for molecules like drugs, nutrients, oxygen, cell wastes within swollen hydrogel, [15] structural similarity to the extracellular matrix of tissues; besides being amenable to relatively mild processing conditions. High water content of hydrogels contributes to the biocompatibility and their soft rubbery property resembles the living tissue.[16] Swollen porous hydrogels can offer a native tissue – a mimicking microenviourment.[17] A variety of synthetic and naturally derived materials have been used to prepare porous hydrogels for tissue engineering scaffolds [18] and their physical, chemical, morphological and biological properties could be tailored for a particular application.

The methods available for synthesis of hierarchically porous materials include gas foaming, [19] phase separation, [20] solvent casting and particle leaching [21] etc. These methods provide good control over the porous architecture but involve multistep complex procedures, which are time consuming. The polymerized high internal phase emulsions (PolyHIPEs) are

[a] *Chemical Engineering and Process Development Division, National Chemical Laboratory, Council of Scientific and Industrial Research (CSIR), Pune – 411008, India.*
[b] *Academy of Scientific and Innovative Research (AcSIR), Council of Scientific and Industrial Research (CSIR), New Delhi, India.*
[c] *Polymer Science and Engineering Division, National Chemical Laboratory, Council of Scientific and Industrial Research (CSIR), Pune – 411008, India.*
[d] *MAEER's Maharashtra Institute of Pharmacy, Kothrud, Pune- 411038, India.*
[e] *Dept. of Chemistry, Savitribai Phule Pune University, Pune- 411007, India.*
* *To whom correspondence should be addressed: ms.qureshi@ncl.res.in*

more recently explored materials as scaffolds.[22-24] PolyHIPEs have been synthesized using high internal phase emulsions (HIPEs) as templates.[25-27] HIPEs are emulsions that have an internal phase volume greater than 74% dispersed in continuous (external) phase. Polymerization of continuous phase of HIPEs gives rise to porous polymers (polyHIPEs) with open cells and interconnected pores after removal of dispersed internal phase [28] that impart excellent mass transport property [29] for oxygen, nutrients, waste metabolite which is necessary for uniform cell migration, cell survival and proliferation.

In recent times, advances in HIPE methodologies have been made to produce porous polymeric materials [23] and the most common being polyHIPE systems synthesized by water-in-oil emulsions route, where the oil phase consists of polymerizable monomers. Several groups have demonstrated the applicability of polyHIPE as scaffold for tissue engineering [30-36] of which the styrene–DVB polyHIPE is the most studied system synthesized by water-in-oil emulsions route. However, these polyHIPEs are intrinsically limited by matrix hydrophobicity and the difficulty in introducing surface functionality to make them hydrophilic by post polymerization modification which is hampered due to the inert nature of polymer and harsh reaction conditions.[37] To overcome the intrinsic hydrophobicity of polyHIPEs synthesized via water-in-oil route, synthesis of hydrophilic polyHIPE was suggested following oil-in-water methodology by using hydrophilic monomers in aqueous (continuous) phase. [38] However, hydrophilic polyHIPEs remain less explored systems for biomedical applications mainly for poor emulsion stability, relatively limited synthesis windows, low porosity and/or poor interconnectivity [23, 39] besides use of toxic organic solvents.

In this study we report the synthesis of superporous polyHIPE hydrogels for tissue engineering applications by copolymerization of glycerol monomethacrylate (GMMA), 2-hydroxy ethyl methacrylate (HEMA) and glycerol dimethacrylate (GDMA) as a cross-linker following inverse (i.e. oil-in-water) HIPE polymerization methodology using non toxic oil phase. So far no study has been reported on the preparation of porous hydrogels based on inverse HIPE polymerization of HEMA, GMMA and GDMA. The co-monomer HEMA was selected for its wide applicability in the biomedical fields.[40-43] In addition, we have also described an alternative facile method for the synthesis of GMMA co-monomer using Amberlyst-15 as a recyclable catalyst.

Experimental Section

Materials

Glycidyl methacrylate (GMA), 2-hydroxy ethyl methacrylate (HEMA), glycerol dimethacrylate (GDMA), Amberlyst-15 (H^+ form) and Triton X-305 (HLB-17.3) were purchased from Sigma Aldrich Chemical Co. (USA) and used as such without further purification. Amberlyst-15 was activated at 120 °C before use. Ammonium persulphate (APS), reducing agent N, N, N', N'-tetra- methylethylenediamine (TEMED) and liquid paraffin oil (light, SF 3S630244) were purchased from Merck (India). The culture of cells NIH3T3 was purchased from National Center for Cell Science (NCCS), Pune (India).

Methods

Synthesis of Glycerol Monomethacrylate

Glycerol monomethacrylate (GMMA) monomer is usually obtained by the reaction of a protected vicinal ketal form of glycerol with methacryloyl chloride followed by acid hydrolysis of the protected ketal group.[44] We have achieved an economical and environment friendly synthesis of GMMA (section 1, ESI) by direct acid-catalyzed hydrolysis of glycidyl methacrylate (GMA) where solid catalyst Amberlyst-15 – a macro-reticular anion exchange resin – was used. The advantages[45] of macro-reticular resin are: its pore size is considerably larger permitting diffusion of reactants freely throughout the resin that makes the functional group ($-SO_3H^+$) available for the catalytic activity, and it is amenable to recycling. The hydrolysis of the epoxy ring of GMA gives mainly of mixture of 2, 3-diol and varying amounts of 1, 3-diol isomers (Fig. S1, ESI) which finally attains an equilibrium concentration of 90:10 respectively on standing for about two weeks.[44, 46]

PolyHIPE preparation

In a typical experiment, the liquid paraffin oil (dispersed phase, 80 vol. % on total volume) was added drop wise to the continuous (aqueous) phase consisting of Triton X-305 (10 % by weight), GMMA and HEMA in various molar concentrations, fixed amounts of cross-linker GDMA (25 mol % of GMMA and HEMA) and initiator APS (2 mol% of monomers and cross-linker) in deionized water (Table 1), while constant stirring at 1000 rpm. After complete addition of the oil phase, the HIPE was further stirred for five min. to improve emulsion uniformity (similar to mayonnaise consistency) and then the reducing agent TEMED (2 mol% of monomers and cross-linker) was added. The HIPE was covered and kept at 37 °C in a water bath for polymerization for 6 h during which cross-linking of polymer chains locked-in the emulsion geometry of HIPE with the suspended oil droplets as a pore template to form the polyHIPE hydrogel. After the polymerization was over, the polyHIPE was washed thoroughly with deionized water and Soxhlet extracted for 12 h with acetone to remove the oil phase. Finally, the resulting polyHIPE was dried overnight to constant weight under vacuum at 65 °C to produce white fluffy hydrogel having physical strength similar to popcorn, and a feel somewhat similar to ethylene-vinyl acetate (EVA) copolymer, but to a degree lighter. The mass balance for dried polyHIPEs and co-monomers including cross-linker matched with in the experimental limits.

Characterization

Mechanical Testing

The static compression test was carried out in a simplified manner on the swollen polyHIPE hydrogels to determine their

mechanical property. The polyHIPE hydrogels test samples were carefully cut into flat rectangular test pieces of about 8×10×5 mm (length × width × thickness) and allowed to swell to the equilibrium state in deionized water for 6 h. The swollen test specimens were kept on a clean glass plate and subjected to a compressive force (F = mg) by gently placing a calibrated mass (m), ensuring that it exerts pressure evenly, and the change in thickness was noted. The thickness of compressed specimens was carefully measured after 5 min. under stress with the help of callipers. The magnitude of compressive stress was calculated (force per unit area, Nm^{-2}) and the resultant compressive strain was determined as $\Delta t/t_0$, where Δt is the change in thickness and t_0 is original thickness. The compressive strain was measured under the static load of 10.32 kPa and the strain recovery was determined by measuring the thickness when the load was removed and the polyHIPE hydrogels samples rested for 5 min. The new sample thickness was divided by the original thickness to calculate the strain recovery. The subsequent strain recoveries were also determined as discussed for three consecutive compressive loading-unloading cycles after resting the samples for 5 min. The new recovered sample thickness after 5 min. was divided by the thickness of the previous cycle to calculate the strain recovery.

Degradation study

In vitro degradation study was conducted by measuring the percent weight loss in 0.007 M NaOH and 1.0 mg mL^{-1} lipase solutions as described.[47]

Details about the degradation study and the other physico-chemical characterization techniques, instrumentation, and biological studies are provided under the ESI, section 2.

Results and Discussion

Synthesis of polyHIPE Hydrogels

In order to synthesize polyHIPE hydrogels as tissue scaffold, one has to carefully select the right methodology, monomers, disperse phase and optimize the parameters. A series of novel superporous polyHIPE hydrogels were synthesized by copolymerizing GMMA, HEMA and GDMA on the inverse (oil-in-water) HIPE template stabilized by Triton X-305 (Scheme 1) with APS/TEMED redox initiation at the physiological temperature. After the polymerization, removal of the oil phase yielded the highly porous materials (GHG-1 to GHG-5) having interconnected open porous architecture with bimodal pore size distribution. The monomers HEMA and GMMA were selected as they have been used for neutral polymeric hydrogels which have found wide applications in biomedical field and GDMA was selected for being hydrophilic and flexible cross-linker. Among many disperse phases e.g. liquid paraffin oil, toluene, xylene, and cyclohexane, the liquid paraffin oil was chosen for its biocompatibility.

The FTIR spectra (Fig. 1) of the polyHIPE hydrogels are in agreement with the polymer structure as expected. The bands at 1220 cm^{-1}, 1740 cm^{-1}, 2954 cm^{-1}, and a broad band centered at 3430 cm^{-1} (range 3149 - 3660 cm^{-1}) are attributed to the presence of C-O, C=O, C-H and OH groups respectively. The absence of the band at 1630 cm^{-1} in the FTIR spectrum of polymer networks indicated that there was no C=C bond unsaturation in the polyHIPE hydrogels. These hydrogels were characterized and found to be promising materials as a scaffold in tissue engineering.

Effect of Surfactant

In general, the choice of surfactant and its quantity determines the emulsion stability and thus HIPE formation.[7] However, for inverse HIPE, the choice of surfactant is critical because of their poor stability.[23] In case of HIPE, surfactant(s) are selected mostly on trial and error basis, besides on the hydrophilic-lipophilic balance (HLB) values; surfactants with the HLB values 2-6 are used for water-in-oil emulsions and 12-16 for oil-in-water emulsions. Therefore, in this work, various high HLB surfactants (HLB>15) such as Tween-40 (HLB, 15.6), Tween-20 (HLB, 16.6), and Triton X-305 (HLB, 17.3) were tried for preparing the inverse HIPE. However, in spite of the comparable HLB values, the most effective surfactant for obtaining stable emulsions turned out to be Triton X-305. This was attributed to the fact that the hydrogen bonding plays a critical role [7] in the stabilization of the HIPE by the surfactant. The surfactants Tween-20 and Tween-40 have more hydrogen bond donor/acceptor sites in the polar head as compared to Triton X-305. Since the monomers and cross-linker also have the hydrogen bond donor/acceptor sites, there was a stronger interaction (H-bonding) between the monomers and the cross-linker and the polar head of the surfactants Tween-20 as well as Tween-40, as compared to Triton X-305. This perhaps prevented the polar head of Tween-20 and Tween-40 from interacting with the aqueous phase of the emulsion and impaired their ability to stabilize the organic/water interface.

Cross-linker concentration

In order to study the effect of cross-linker concentration in the continuous phase for obtaining stable emulsion with desired morphology, the polyHIPE hydrogels were synthesized with 1, 5, 10 and 25 mole percent concentration of GDMA while keeping the rest of the composition including the monomers concentration fixed (GMMA:HEMA, 100:0). It was observed that the polyHIPE morphology progressively improved from almost nonporous to highly porous as the cross-linker concentration increased. At 1 mol% concentration of GDMA almost no porosity developed (Fig. 2A) and only rudimentary porosity (with very irregular pore shape and without pore interconnectivity) started emerging at 5 mol% concentration (Fig. 2B). As the concentration of the cross-linker was increased to 10 mol%, the porosity of the polyHIPE improved further (the pore shape became better) but with thicker pore walls and fewer interconnects (Fig. 2C). At 25 mol% GDMA concentration a polyHIPE hydrogel with desired porous structure and having highly interconnected open-pore architecture resulted (Fig. 2D). Therefore, all the polyHIPE hydrogels, reported in this work, were synthesized keeping the crosslink density at 25 mol%.

Concentration of cross-linker can impact the emulsion stability and affect the morphology of polyHIPE by altering the cross-linking kinetics, which depends on the number of cross-linking sites available besides the reactivity of the double bond.[48] In our case, the gradual increase in GDMA concentration resulted in larger number of the cross-linking sites (double bonds) available which in turn enhanced the rate of cross-linking and hence produced the stable emulsion leading to a polyHIPE hydrogel with the progressively improved and finally the desired morphology.

Effect of molar ratio of monomers

Initially, we tried to synthesize the superporous hydrogel of HEMA by the inverse HIPE methodology using GDMA as a cross-linker but the emulsion was not stable. The co-monomer GMMA was incorporated in the formulation along with HEMA in different mole ratios (Table 1) and it was noted that the addition of GMMA vastly improved the emulsion stability. Further, we observed that when the molar ratio of GMA: HEMA was increased beyond 40:60, the emulsions were not stable. The change in the emulsion stability was confirmed by the optical microscopy (Axioscope-A1, Carl Zeiss, Germany) by gently casting the emulsion on silanized glass plate. When the emulsions were stable the optical microscopic images showed that the emulsion droplets were uniformly distributed (Fig. S2A, ESI) but when the emulsion stability started decreasing there was an uneven distribution or deformation of the emulsion droplets (Fig. S2B, ESI). Since GMMA played a very important role in stabilizing the emulsions, the polyHIPE hydrogels were synthesized with the composition of GMA: HEMA by restricting the range from 100:0 to 40:60 while the molar concentration of the GDMA cross-linker was kept constant at 25 mol % as discussed above.

Initiator

The phase separation of the emulsion occurred either when the polymerization was initiated at the locus of the aqueous phase thermally with ammonium persulphate (APS) at the elevated temperatures (>50°C) or when benzoyl peroxide was employed to initiate the polymerization at the locus of organic phase. Subsequently, we tried the redox initiated polymerization at the physiological temperature (37 ^{o}C) at the locus of aqueous phase by using water soluble initiator APS as an oxidizing agent and TEMED as an accelerator. The redox initiated polymerization produced highly porous polyHIPE hydrogels having interconnected open-pore architecture. It may be noted that the open pore interconnectivity of the polyHIPE was achieved only with the organic phase initiation as reported by Robinson et al.[7] and when they used the aqueous phase initiation the closed pore morphology was observed. However, this study, with the aqueous phase initiation, demonstrated that the organic phase initiation was not a necessity for producing open pore interconnected polyHIPE hydrogels. In addition, the APS-TEMED redox initiation allowed the increased cure rate at the physiological temperature that makes this system potentially viable for *in situ (in vivo)* polymerization.

Porous structure and mechanical properties

The concentration of HEMA and GMMA were varied to examine the effect of composition on the morphology and the properties of the polyHIPE hydrogels. The SEM images (Fig. 3) show that all the hydrogels exhibited open porous bimodal morphologies with high porosity ranging from 92.3% to 96.6% (Table 2) that is typical of the polyHIPE porous structures.[49] The surface area of the polyHIPE hydrogels varied between 2.89 and 23.1 $m^2 g^{-1}$ (Table 3). With the increased proportion of HEMA up to 60 mol% in the copolymer, the porosity of hydrogels increased (consequently, the surface area and the pore volume, too), whereas the pore size, pore throat size and pore wall thickness decreased (Table 2). This led to the formation of relatively stiffer (GHG-1) to softer (GHG-5) hydrogels as indicated by the decreasing trend in the glass transition temperature (T_g) and the increasing trend in the % compression (Table 4). The pore and pore throat sizes as well as the pore wall thickness of these hydrogels were determined from the SEM images using Image J software (Image J 1.46). The field of the SEM images was divided into equal quadrants and more than 30 numbers of pores, pore throats and pore walls each were selected randomly from every quadrant for calculating the average and the standard deviation.

The pore throats or pore interconnect formation takes place due to the shrinkage of the thin polymer film (separating droplets) during the polymerization as well as during the post polymerization process of Soxhlet extraction and drying. As a result, the pore throat size was expected to decrease with the increase in the pore wall thickness. However, contrary to the expectation, the pore throat size increased with the increase in the pore wall thickness. Similar results have been reported for the polyHIPEs obtained by the inverse HIPE methodology. [50] All the polyHIPE hydrogels were amenable to repeated complete drying and full recovery of their water content on re-immersion in water indicated that they have an open interconnected pore structure. [51]

The HIPE emulsions underwent some coalescence (droplet coarsening) indicated by the presence of the larger secondary pores compared to the basic or primary pores in the polyHIPE hydrogels. The basic or primary pores formed during the emulsification stage morphed into the larger secondary pores through the coalescence during the polymerization process. [48] The size and frequency of coalesced pores is inversely proportional to the stability of HIPE. For 60 mol% HEMA in the co-polymer (GHG-5) the size and the number of coalesced pores increased (Fig. 3E) and beyond this composition (60 mol% HEMA) the HIPEs were unstable.

The water swelling ratio (Table 3) and the pore volume increased with the decrease in the pore size (i.e. increase in the porosity) and showed a quadratic fit (Fig. 4A), whereas the pore volume and the mercury intrusion volume showed a linear relationship (Fig. 4B), as expected.

The polyHIPE hydrogels studied, exhibited high porosity (>92%) and the bimodal pore morphology comprised of 19.6-30.3 µm pores and 3.7-7.6 µm interconnecting pore

throats distributed uniformly (which is necessary to facilitate the diffusion of nutrient and waste besides uniform distribution of cells by promoting their migration), can be used for soft tissue engineering applications. Many attempts have been made to determine the ideal pore size of scaffold for tissue engineering applications but without any clear consensus; often the results are contradictory or may be specific to cell type. [52] In general, the pore sizes >100 µm are considered suitable for this purpose.[53] However, for tissue engineering scaffolds, pore sizes 1.4-7.3 µm have also been described[50] and recent studies indicate that <40 µm pores improve tissue regeneration. [53]

None of the polyHIPE hydrogels shrunk and crumpled or collapsed during the drying step. This was partly because of relatively high degree of cross-linking (25 mol% GDMA) and partly due the lower glass transition temperature that reduced the stiffness and decreased the resistance to the stress generated during drying, as also observed by Gitlli and Silvestein.[51] The compressive strain and the initial strain recovery increased with decreasing GMMA and increasing HEMA contents for all the PolyHIPE hydrogels. The hydrogel having 100% GMMA (GHG-1) was the stiffest composition tested, with a compressive strain of 25.0 when 10.32 KPa load was applied and showed an initial strain recovery of 80.7% on the load removal. These values increased steadily to 41.9 and 92.2% as GMMA concentration decreased to 40% and HEMA increased to 60%. The mechanical properties and the structural integrity of the scaffolds were mainly determined by the porous morphology (e.g. porosity, pore and pore throat size, pore wall thickness and pore volume); crystallinity, discussed under thermal properties, contributed to a very small extent.

With the increased porosity, the polyHIPE hydrogels became increasingly softer as indicated by the increase in the compressive strain. The compressive strain and the initial strain recovery are inversely related to the pore size (as well as the pore throat size, and the pore wall thickness) and these data showed a quadratic fit (Fig. 5A and 5B). The compressive strain and the initial strain recovery data for GHG-1 to GHG-5 showed a linear relationship (Fig. 5C) indicating the softer hydrogels recovered better.

The initial strain recovery increased with increased HEMA content, and approached 92% upon subsequent loading which indicated the ability of these scaffolds to recover from the strain. The 100% GMMA (GHG-1) exhibited the lowest initial recovery (80.7%), and the highest recovery was shown by GHG-5 (92.2%).

Swelling kinetics in water

A study of the swelling behaviour of the polyHIPE hydrogels was carried out in water since the wettability and the swelling are very important properties of a scaffold for tissue engineering. The scaffold's wettability determines the cell seeding and proliferation [50] whereas the swelling is responsible for the nutrient transport[54] to (and removal of toxic metabolites from) the cells growing on the polymer matrix. It was observed (Fig. S3, ESI) that the swelling of all the five polyHIPE hydrogels took place very rapidly and reached the equilibrium swollen state in around 10 min. However, the swelling ratio (*Q*) given in Table 3 were determined after 4 h. The highest value of *Q* (13.6 ± 0.05) was observed for GHG-5 (GMMA: HEMA, 40:60), whereas GHG-1 (100% GMMA) showed the lowest values of *Q* (8.1 ± 0.05).

As was expected, the swelling ratio increased as the hydrophilicity (total no of –OH groups in the polymer, calculated assuming complete polymerization indicated by mass balance for the dried polyHIPEs and comonomers including the cross-linker) and the porosity of polyHIPE increased (Table 3). In addition, the swelling parameters (*Q*) also increased with increase in the surface area. This could be due to the higher percentage of –OH groups became accessible to the surrounding water molecules for the interaction through the hydrogen bonding. Indeed, the correlation (Fig. 4C) of *Q* with the hydrophilicity (total no of –OH groups in the polymer) improved vastly (Fig. 4D) when the surface area was applied as the weight factor by multiplying it with the total no. of -OH groups, to determine the corrected hydrophilicity.

Thermal properties

The thermal characteristics of the polyHIPE hydrogels were studied with the help of DSC and TGA (Table 4). In the DSC thermograms for the polyHIPE hydrogels (Fig. 6) both the T_g and the melting endotherm peak (T_m) are observed. With the increased HEMA and the decreased GMMA contents, the T_g decreased and the T_m shifted towards the lower temperature initially slowly for GHG-1 (131.9 ^{o}C) to GHG-3 (130.6 ^{o}C) and rapidly for GHG-4 (122.8 ^{o}C) to no melting endotherm for GHG-5. This endotherm indicated the existence of a small amount of crystallites which was also substantiated by X-Ray diffraction patterns (neither very sharp nor completely diffused, Fig. S4, ESI), in GHG-1 to GHG-4. Similar observation on small amount of the crystallites was made for other polyHIPE having 22 mol% ethylene glycol dimethacrylate (EGDMA) as a cross-linker, [55] which is flexible and resembles to GDMA used in this work. When flexible cross-linker e.g. GDMA (or EGDMA) is employed, chain segments with relatively low cross-link densities and, consequently, relatively unrestricted molecular mobility, can organize themselves into the more ordered crystalline domains that results into the melting endotherm.[55] In addition, the formation of these crystalline domains is assisted by the intra molecular (intra chain) hydrogen bonding between –OH groups as evidenced by a broad O-H stretching band centered around 3430 cm^{-1} (range 3149 - 3660 cm^{-1}) in the FTIR spectrum (Fig. 1). Based on the above data and the discussion, a representative amorphous-crystalline schematic model (Fig. 7) is proposed. The model shows that the polyHIPE hydrogels (GHG-1-GHG-4) are predominantly amorphous with the little crystallinity. However, GHG-5 did not show any discernible crystallinity.

The decrease in the T_m indicated reduction in the degree of crystallinity in GHG-1 to GHG-4 and for GHG-5 there was no discernible crystalline region since no T_m was observed. In

addition, concomitant to the T_m, the T_g also decreased with the reduction in the degree of crystallinity. As a consequence of the decreased degree of crystallinity, the density (d) of the polymer is expected to decrease for less compact packing of the molecular chains (mass) in a given volume. Indeed, the T_g decreased with the decrease in density (d) of the polymer (determined after grinding the polyHIPE hydrogels to fine powder to remove the porosity) and showed a perfect (r^2=1) 3rd degree polynomial (cubic) correlation (Fig. 8A). The lowering of the T_g was also consistent with the reduced stiffness (increased compression) of GHG-1 to GHG-5 (Table 4) which reduced the resistance to the stress generated during the drying and thus helped in maintaining the dimensional integrity. [51]

The TGA and DTG curves (Fig. S5, ESI) show the thermal degradation of the polyHIPE hydrogels. All the samples except GHG-1 degraded in the three stages viz., the small shoulders at around 200 °C (corresponding weight loss, 2-4 %) and 275 °C (corresponding weight loss, 8-10 %) and the main (dominant) degradation peak at 411.2 ± 5.0 °C (corresponding weight loss, 69-72 %) and a residual mass of 7-8 % at about 450 °C. In addition to three DTG peaks, the main degradation peak of GHG-1 showed an additional shoulder at around 350 °C (corresponding weight loss, ~30 %) and the degradation peak at 411.2 °C (corresponding weight loss, ~40 %). The weight loss onset temperature of the main peak decreased with the increased HEMA and the decreased GMMA contents. Further, it was noted that the peak (before 100 °C) due to the loss of moisture, shifted towards the lower temperature (Table 4 and Fig. S5, inset, ESI) from GHG-1 to GHG-5. This was attributed to the increased porosity (surface area) which facilitated relatively easy removal of water from the hydrogels; consequently, the moisture peak shifted to the lower temperature. The weight loss onset temperature showed a similar cubic correlation (Fig. 12B) with the density (d) as that of the T_g, albeit less than perfect (r^2=0.9873). Therefore, the T_g and the weight loss onset temperature showed a linear correlation (r^2=0.9886), which was expected (Fig. 8C). As the polyHIPE hydrogels became denser, the onset degradation temperature, T_g and T_m increased. However, the variation in T_m was not pronounced but fairly discernible.

Degradation

The synthesized polyHIPE hydrogels were subjected to the accelerated degradation at room temperature in 0.007 M sodium hydroxide solution to test that the hydrolytically labile ester bonds are accessible by monitoring the % mass loss on 2nd, 5th and 10th day. All the hydrogels showed the linearly increasing degradation (slope, 1.8727 ± 0.0599 and r^2 > 0.997) (Fig. 9) with an average % mass loss of 7.2 ± 0.6 (2-days), 12.0 ± 0.3 (5-days) and 22.0 ± 0.3 (10-days), except GHG-1. The average % mass loss for GHG-1 after 2 days was same (7.2 ± 0.6) as those of rest of the four hydrogels but increased to 14.1± 0.6 (5-days) and 26.0 ± 0.3 (10-days). Since all the hydrogels had fixed cross-linking degree at 25% they were expected to degrade with the same rate including GHG-1.

The higher rate of degradation of GHG-1, though marginal but discernible (Fig. 9), can be rationalized by hypothysing that the hydrolysis of the ester bonds in the hydrogels takes place via the base catalyzed bimolecular acyl cleavage ($\mathbf{B_{AC}2}$) mechanism which is the most common under strong basic condition where the OH^- nucleophile directly attacks the electrophilic carbon (>C=O) of the ester and breaks the π bond to form the tetrahedral intermediate leading to organic acid and alcohol formation.[56] Further, the nucleophilic attack of OH^-, which is the rate determining step (RDS), will be facilitated if the electrophilic carbon (>C=O) is attached with an electron withdrawing group(s) and the overall rate of reaction will increase. There is only one electron withdrawing –OH group in the polymer chains due to HEMA and GDMA whereas chain due to GMMA has two –OH groups (scheme 1). Furthermore, GMMA has two positional isomers (Scheme S1, ESI) of which 1,3-hydroxy GMMA (13%) could be more susceptible to hydrolysis as both the electron withdrawing –OH groups are closer to the electrophilic carbon (>C=O) than 2,3-hydroxy GMMA (87%).

Since the polyHIPE hydrogel GHG-1 had 100% GMMA, it was more susceptible to hydrolysis and showed the higher rate of degradation. It may be noted that the higher degradation rate of GHG-1 became noticeable only after 5-days which further enhanced (differentiated) on 10th day. The other hydrogels particularly GHG-2 and GHG-3 with relatively higher GMMA content (80 and 60%, respectively) were also expected to show the enhanced rate of degradation than GHG-4 and GHG-5 in the order GHG-1 > GHG-2 > GHG-3 but did not show any discernible change on the experimental timescale of 10 days. In principle, it would be expected and interesting to see if GHG-2 and GHG-3 show the enhanced rate of degradation in the expected order on the longer timescales.

In order to examine the degradability in biological environment, degradation of GHG-5, as a representative case, in 1.0 mg L^{-1} lipase B (*Candida antarctica*) solution was studied in a similar ways as that of the degradation in 0.007 M NaOH. The mass loss for the hydrogel, unlike in 0.007 M NaOH, was not only much lower i.e. 1.0% (2-days), 7.0% (5-days) and 8.4% (10-days), but also did not vary linearly with time. This may be due to the diffusion of the enzyme lipase, into the bulk of the hydrogel, is limited by the size of the enzyme. [47]

It was observed that all the hydrogels disintegrated in 0.007 M NaOH after 10 days whereas in 1.0 mg L^{-1} lipase B solution there was no noticeable change in the integrity of the material. This showed that the relatively extensive surface as well as the bulk degradation of the hydrogels took place in the NaOH solution as compared to the lipase solution.

Biocompatibility

Cytotoxicity

In vitro cytotoxicity evaluation is the first step towards the biocompatibility of materials. In order to investigate the potential of the polyHIPE hydrogels as a scaffold for tissue engineering, assessment of their biocompatibility was carried out using a well characterized NIH3T3 cell line. The cell viability was assessed for 5 days relative to TCPS as cytocompatible control. The assessment indicated that the hydrogels exhibited

greater than 97 % cell viability after 5 days (Fig. 10). The images of NIH3T3 cells in the presence of hydrogels and the control after 5 days are shown (Figure S6, ESI). It was noted that there was no significant difference in the cell viability as compared to TCPS. The cytotoxicity study indicates that these hydrogels are not toxic and hence taken up for cell adhesion and proliferation study.

Cell adhesion and proliferation

The cell adhesion and proliferation study was carried out as discussed under ESI, section 2. The assessment revealed that the polyHIPE hydrogel samples exhibited greater than 55 % cell viability after 7 days (Fig. 11). In all the polyHIPE hydrogels there was a homogeneous distribution of the pores and interconnecting windows (pore throats) necessary to facilitate the diffusion of nutrients and waste metabolites which led to a growth and migration of the cells from the site of seeding. Though the hydrogels did not show any significant toxicity (97% cell viability), but, in comparison, the cell proliferation data showed much less cells viability (55-88%) in cell adhesion and proliferation study. This could be because of modulation of the physical and chemical properties of these hydrogels with the cell growth.

After day one, the average % viable cells on all the PolyHIPE hydrogels was 95.6 ± 2.9 as compared to TCPS (100 ± 1.8 %), while after seventh day, GHG-1 and GHG-5 showed 56.6 ± 1.7% and 88.4 ± 4.2 % cell viability respectively relative to TCPS (100 ± 3.8 %). The % cell viability on the polyHIPE hydrogels increased monotonously from GHG-1 to GHG-5 and correlated well with their physical and chemical properties as expected. The increase in % cell viability could be attributed to the increase in porosity (i.e. decrease in pore and pore throat size), pore volume, surface area, area to volume ratio and hydrophilicity (Fig. 12). The increasing hydrophilicity (increased –OH groups and increased surface area) of the polyHIPE hydrogels promoted the cell adhesion, migration and proliferation of the seeded cells.[38] Klouda et al. reported that cell viability greater than 75% is necessary for a material to be biocompatible.[57] However, materials having cell viability up to about 40% is also reported as biocompatible.[58] The phase contrast microscopic images (Fig. S7, ESI) show the continual increasing trend in the cell viability from GHG-1 to GHG-5; whereas, the florescence microscopy (Fig. 13) clearly show that the number of live cells (green) increased and the dead cells (red) decreased. The cells were spread with elongated morphology retaining their nuclear integrity which is a sign of healthy and proliferating cells. These results confirm the cytocompatibility of the polyHIPE hydrogels and their ability to support cell proliferation.

For tissue engineering applications porous scaffold with pore size ranging from 4 µm to 100 µm have been used depending on the scaffold function and types of cells to be repaired.[50,53] Recently, Krajnc et al. have reported the porous monoliths with pore size 20 µm for the culture of osteoblasts[24] and gelatin – PHEMA based scaffolds with pore size from 30 µm to 215 µm have shown 40 to 60 % cell viability.[58] In comparison to these results, our materials, prepared by varying the monomer ratio, have intrinsic hydrophilicity and pore size in the range of 20 µm to 40 µm, showed better cell viability (55-88 %). In addition, the inverse HIPEs reported in this study were stable enough and form the interconnected porous architecture as compared to the i-HIPE studied earlier.[23,39] Therefore, the polyHIPE hydrogels prepared via inverse HIPE route in this work are considered promising materials as tissue scaffold.

Conclusion

In this work, a series of superporous polyHIPE hydrogels were successfully synthesized by inverse high internal phase emulsion polymerization (i-HIPE) of the water soluble monomers, cross-linker at the physiological temperature using a non toxic organic solvent as dispersed phase. The morphology and the properties of the materials could be altered by changing the monomer ratio. The described materials showed sufficiently high swelling ratio, porosity, hydrophilicity and thereby increased degradability and improved biocompatibility. The open porous morphology - a key design criterion for tissue scaffold - of the reported polyHIPE hydrogels permitted fast enough convective mass transport of nutrients and oxygen which resulted in the cell growth and proliferation. In addition, these polyHIPE hydrogels exhibited desired mechanical properties viz., compressive strain, strain recovery and dimensional integrity on drying at 65 °C - a temperature higher than the human body temperature. Assessment of in vitro cell adhesion and proliferation has shown that these materials supported the cell adhesion, their penetration and proliferation. Overall, the described polyHIPE hydrogels resembled to many of soft tissues of the human body, and therefore can be considered as promising materials for tissue scaffolding. In addition, APS-TEMED redox initiation allowed increased cure rate and quicker development of porous interconnect network at physiological temperature and thus could be potentially viable for *in situ* (*in vivo*) polymerization, as well.

Acknowledgements

We are thankful to the Director, National Chemical Laboratory for providing necessary facilities and to the Council of Scientific and Industrial Research (CSIR), New Delhi, India for providing senior research fellowship to one of us (ACN). Thanks are also due to Ms Sonali M. Bhosle for the help in synthesizing GMMA monomer used in this work. Thanks are due to Dr. M. S. Shashidhar for the critical review of the manuscript.

Notes and references

[1] F. O'Brien, *Materials Today,* 2011, **14**, 88-95.

[2] B. Dhandayuthapani, Y. Yoshida, T. Maekawa and D. Kumar, *International Journal of Polymer Science,* 2011, **2011**, 1-19.

[3] S. J. Hollister, *Nat. Mater.,* 2005, **4**, 518-524.

[4] N. Annabi, J. Nichol, S. Zhang, C. Ji, S. Koshy, A. khademhosseini and F. Dehghani, *Tissue Engineering B*, 2010, **16**, 371-383.
[5] R. Ravichandran, S. Sundarrajan, J. Venugopal, S. Mukherjee and S. Ramakrishna, *Macromolecular Bioscience,* 2012, **12**, 286-311.
[6] R. Moglia, J. Holm, N. Sears, C. Wilson, D. Harrison and Cosgriff Hernandez, *Biomacromolecules*, 2011, **12**, 3621-3628.
[7] J. Robinson, R. Moglia, M. Stuebben, M. McEnery and E. Cosgriff-Hernandez, *Tissue engineering A*, 2014, **20**, 1103-1112.
[8] Q. Hou, P. Bank and K. Shakesheff, *J. Mater. Chem.*, 2004, **14**, 1915-1923.
[9] J. Kretlow, L. Klouda and A. Mikos, *Advanced Drug Delivery Reviews,* 2007, **59**, 263-273.
[10] O. Wichterle, Hydrogels, In: Encyclopedia of polymer Science and Technology, H.F. Mark, N. G. Gaylord, N. Bikanes, eds., Interscience, Vol. 15. New York, 1971, pp. 273-291.
[11] D. Seliktar, *Science*, 2012, **336**, 1118-1124.
[12] S. Varghese and J. Elisseeff, *Adv. Polym. Sci.,* 2006, **203**, 95-144.
[13] A. Hoffman, *Advanced drug delivery reviews*, 2002, **54**, 3-12.
[14] K. J. R. Lewis and K. S. Anseth, *MRS Bull.,* 2013, **38**, 260-268.
[15] N. A.Peppas, J. Z. Hilt, A. Khademhosseini and R. Langer, *Adv. Mater.,* 2006, **18**, 1345-1360.
[16] A. Ovsianikov, A. Deiwick, S. V. Vlierberghe, P. Dubruel, L. Moller, G. Drager and B. Chichkov, Biomacromolecules, 2011, **12**, 851-858.
[17] M. Parlato, S. Reichert, N. Barney and W. L. Murphy, *Macromol. Biosci.,* 2014, **14**, 687-698.
[18] S. V. Vlieberghe, P. Dubrue and E. Schacht, *Biomacromolecules,* 2011, **12**, 1387-1408.
[19] B. S. Kim and D. J. Mooney, *Trends Biotechnology*, 1998, **16**, 224-230.
[20] C. Tu, Q. Cai, J. Yang, Y. Wan, J. Bei and S. Wang, *Polymers for Advanced Technologies*, 2003, **14**, 565-573.
[21] Q. Hou, D. Grijpma and J. Feijen, *Biomaterials*, 2003, **24**, 1937-1947.
[22] R. Moglia, M. Whitely, P. Dhavalikar, J. Robinson, H. Pearce, M. Brooks, M. Stuebben, N. Cordner and E. Cosgriff-Hernandez, *Biomacromolecules*, 2014, **15**, 2870-2878.
[23] M. S. Silverstein, *Polymer*, 2014, **55**, 304-320.
[24] M. Susec, R. Liska, G. Russmuller, J. Kotek and P. Krajnc, *Macromol. Biosci.,* 2015, **15**, 253-261.
[25] H. Zhang and A. Cooper, *Soft Matter,* 2005, **1**, 107-113.
[26] J. M. Williams, *Langmuir,* 1991, **7**, 1370-1377.
[27] T. Gitli and M. S. Silverstein, *Polymer,* 2011, **52**, 107-115.
[28] I. Pulko and P. Krajnc, *Macromol. Rapid Commun.,* 2012, **33**, 1731-1746.
[29] P. Krajnc, N. Leber, D. Stefanec, S. Kontrec and A. Podgornik, *Journal of chromatography A,* 2005, **1065**, 69-73.
[30] G. Akay, M. Birch and M. Bokhari, *Biomaterials,* 2004, **25**, 3991-4000.
[31] M. Bokhari, G. Akay, S. Zhang and M. Birch, *Biomaterials* 2005, **26**, 5198-5208.
[32] A. Barbetta, M. Dentini, M. S. DeVecchis, P. Filippini, G. Formisano and S. Caiazza, *Adv.Funct.Mater.,* 2005, **15**, 118-124.
[33] A. Barbetta, M. Massimi, L. Devirgiliis and M. Dentini, *Biomacromolecules,* 2006, **7**, 3059-3068.
[34] Y. Lumelsky, J. Zoldan, S. Levenberg and M. S. Silverstein, *Macromolecules,* 2008, **41**, 1469-1474.
[35] A. Hayward, N. Sano, S. Przyborski and N. R. Cameron, *Macromol.Rapid Commun.,* 2013, **34**, 1844-1849.
[36] A. Hayward, A. Eissa, D. Maltman, N. Sano, S. Przyborski and N. R. Cameron, *Biomacromolecules,* 2013, **14**, 4271-4277.
[37] N. R. Cameron, D. C. Sherrington, I. Ando and H. Kurosu, *Journal of Materials Chemistry,* 1996, **6**, 719-726.
[38] P. Vishwanathan, S. Chirasatitsin, K. Ngamkham, A. j. Engler and G. Battaglia, *J. Am. Chem. Soc.,* 2012, **134**, 20103-20109.
[39] Z. Li, M. Xiao, J. Wang and T. Ngai, *Macromol. Rapid Commun., 2013,* **34**, 169-174.
[40] X. Lou, S. Munro and S. Wang, *Biomaterials,* 2004, **25**, 5071-5080.
[41] G. H. Hsiue, J. A. Guu and C. C. Cheng, *Biomaterials,* 2001, **22**, 1763-1769.
[42]O. Wichterle and D. Lim, *Nature*, 1960, **185**, 117-118.
[43] S. Kovacic, D. Stefanec and P. Krajnc. *Macromolecules,* 2007, **40**, 8056-8060.
[44] S. E. Shaw, T. Russo, D. H. Solomon and G. G. Qiao, *Polymer,* 2006, **47**, 8247-8252.
[45] Ion Exchange Resins, 6th edn. (Revised), 1988, product no. 570204G, BDH, England, pp.55.
[46] N. Garcia, J. Guzman and E. Riande, *Macromol. Chem. Phys.,* 2002, **15**, 2225-2231.
[47] S. Atzel, S. Curtin, P. Trinh, S. Bryant and B. Ratner, *Biomacromolecule,* 2008, **9**, 3370-3377.
[48] E. M. Christenson, W. Soofi, J. L. Holm, N. R. Cameron and A. G. Mikos, *Biomacromolecules,* 2007, **8**, 3806-3814.
[49] M. Tang, M. Purcell, J. A. M. Steele, K-Y. Lee, S. McCullen, K. M. Shakesheff, A. Bismarck, M. M. Stevens, S. M. Howdle and C. K. William, *Macromolecules,* 2013, **46**, 8136-8143.
[50] S. Zhou, A. Bismark and J. H. G. Steinke, *Macromol. Rapid Commun.,* 2012, **33**, 1833-1839.
[51] T. Gitli and M. S. Silverstein, *Soft Matter,* 2008, **4**, 2475-2485.
[52] R. S. Moglia, J. L. Robinson, A. D. Muschenborn, T. J. Touchet, D. J. Maitland and E. Cosgriff- Hernandez, *Polymer,* 2014, **55**, 426-434.
[53] R. S. Moglia, M. Whitely, P. Dhavalikar, J. Robinson, H. Pearce, M. Brooks, M. Stubben, N. Cordner and E. Cosgriff-Hernandez, *Biomacromolecule,* 2014, **15**, 2870-2878.
[54] A. L. Gatta, C. Schiraldi, A. Esposito, A. D. Agostino and A. D. Rosa, *J. Biomed Mater Res A,* 2009,**90**, 292-321.
[55] S. Livshin and M. S. Silverstein, *Soft Matter,* 2008, **4**, 1630-1638.
[56] J. March, Advanced Organic Chemistry: Reactions, Mechanisms and Structure, 2nd edn. McGraw-Hill, 1977, pp. 349.
[57] L. Klouda, M. C. Hacker, J. D. Kretlow and A. G. Mikos, *Biomaterials,* 2009, **30**, 4558–4566.

[58] D. M. Dragusin, S. V. Vlieberghe, P. Dubruel, M. Dierick, L. V. Hoorebeke, H. A. Declercq, M. M. Cornelissen and I. C. Stancu, *Soft matter*, 2012, **8**, 9589-9602.

Table 1.Composition of inverse HIPE formulations

Sample	GMMA (mM)	HEMA (mM)	GDMA (mM)	APS (mM)	TEMED (mM)
GHG-1	8.324	0	2.081	0.166	0.332
GHG-2	6.658	1.664	2.081	0.166	0.332
GHG-3	5.827	3.885	2.427	0.194	0.388
GHG-4	5.827	5.826	2.913	0.233	0.466
GHG-5	4.994	7.492	3.121	0.249	0.499

Table 2.Characteristics of polyHIPE hydrogels

Sample	Porosity (%)	Pore size [a] (μm)	Pore throat size [a] (μm)	Pore wall [a] (μm)	Hg intr. vol. (cc g^{-1})	Pore vol. (cc g^{-1})
GHG-1	92.3	30.3 ± 7.2	7.7 ± 2.0	1.8 ± 0.3	7.0	5.0
GHG-2	95.3	25.4 ± 8.5	6.2 ± 1.7	1.2 ± 0.4	8.2	5.2
GHG-3	95.2	21.3 ± 6.5	4.6 ± 1.2	0.8 ± 0.1	9.8	5.9
GHG-4	94.9	20.7 ± 6.0	4.0 ± 0.9	0.7 ± 0.2	10.9	6.0
GHG-5	96.6	19.6 ± 5.8	3.7 ± 0.5	0.5 ± 0.6	12.8	7.5

[a] Calculated from SEM images with the help of Image J 1.46 s/w by randomly selecting more than 125 pores(refer text).

Table 3.Physico-chemical properties of polyHIPE hydrogels

Sample	Surface area (m^2 g^{-1})	No. of –OH groups [a] × 10^{-21}	Surface area to volume ratio (m^{-1})	Swelling ratio (Q)	Cell viability [b] (%)
GHG-1	2.89	11.28	41.3	8.1 ± 0.05	56.6 ±1.7
GHG-2	3.43	10.25	41.8	9.1 ± 0.1	58.2 ± 3.3
GHG-3	4.67	10.82	47.7	10.7 ± 0.1	65.2 ± 4.4
GHG-4	10.0	12.28	91.7	11.7 ± 0.05	77.3 ± 2.2
GHG-5	23.1	12.32	180.5	13.6 ± 0.05	88.4 ± 4.2

[a] See text for calculation of number of –OH group.
[b] Number of viable cells as determined by MTT assay after 7 days.

Table 4.Thermal and mechanical properties of polyHIPE hydrogels

Sample	T_g (°C)	T_m (°C)	Onset temp. (°c)	Water peak temp. (°c)	Bulk density [a] (g cc^{-1})	Comp. strain [b] (%)	Strain recov. (%)
GHG-1	7.43	131.9	446	52.7	0.114	25.0	80.7
GHG-2	- 5.35	131.4	412	48.0	0.104	29.4	83.0
GHG-3	- 10 46	130.6	402	53.0	0.095	32.0	85.5
GHG-4	- 10.93	122.8	394	46.0	0.094	35.8	86.0
GHG-5	- 13.51	-	390	43.0	0.064	41.9	92.2

[a] Bulk density determined after crushing hydrogels to fine powder.
[b] Under 10.32 kPa load.

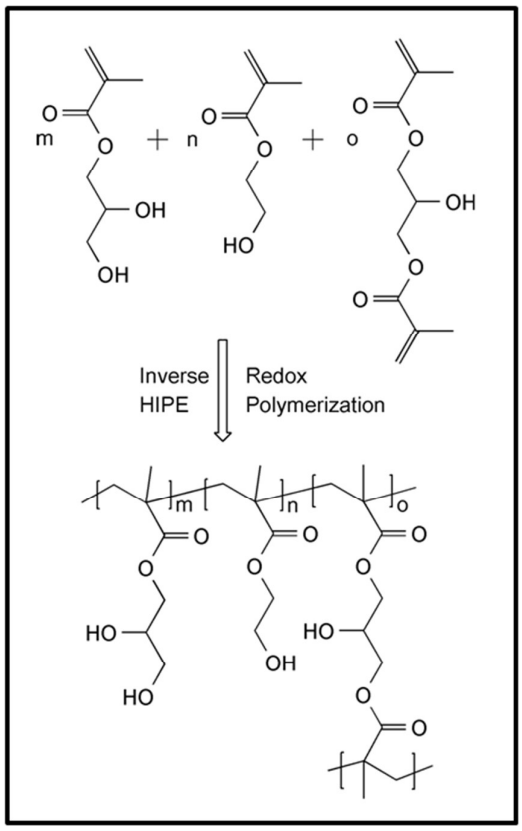

Scheme 1. Copolymerization of GMMA, HEMA and GDMA.

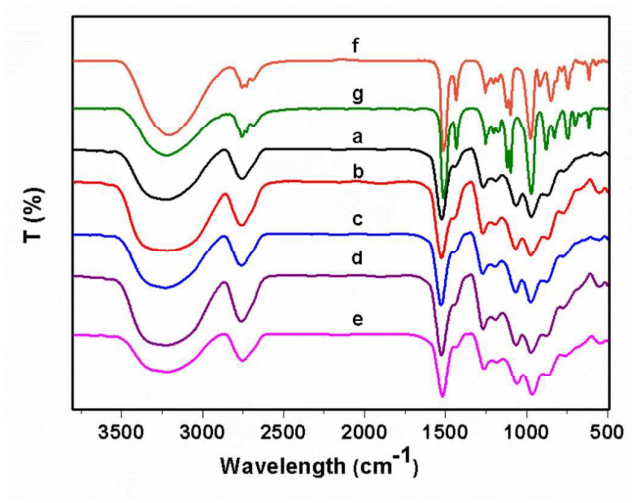

Fig. 1 FTIR spectra of polyHIPE hydrogels: a) GHG-1, b) GHG-2, c) GHG-3, d) GHG-4, e) GHG-5; and monomers: f) HEMA and g) GMMA. (It may be noted that the -OH stretching peak (3149 – 3660 cm^{-1}) is relatively broad in polyHIPE hydrogels as compared to the monomers indicating increased H-bonding).

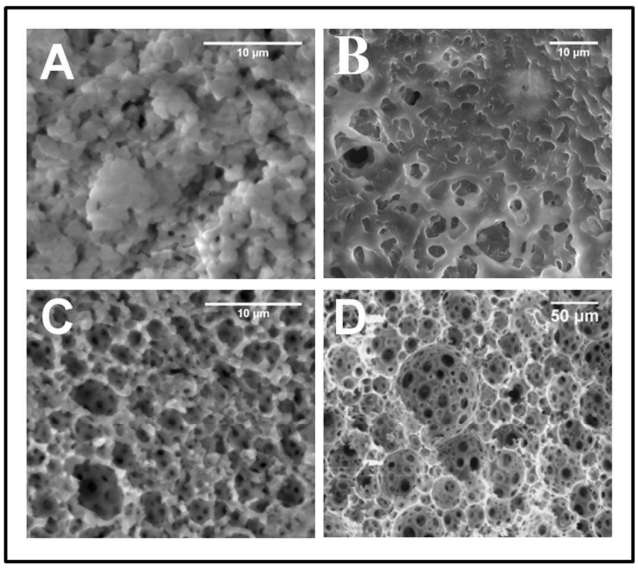

Fig. 2 SEM microscopic images showing the effect of cross-linker concentration on polyHIPE hydrogel morphology; (GMMA:HEMA,100:0) and GDMA: A)1 mol %, B)5 mol %, C)10mol % and D) 25 mol %.

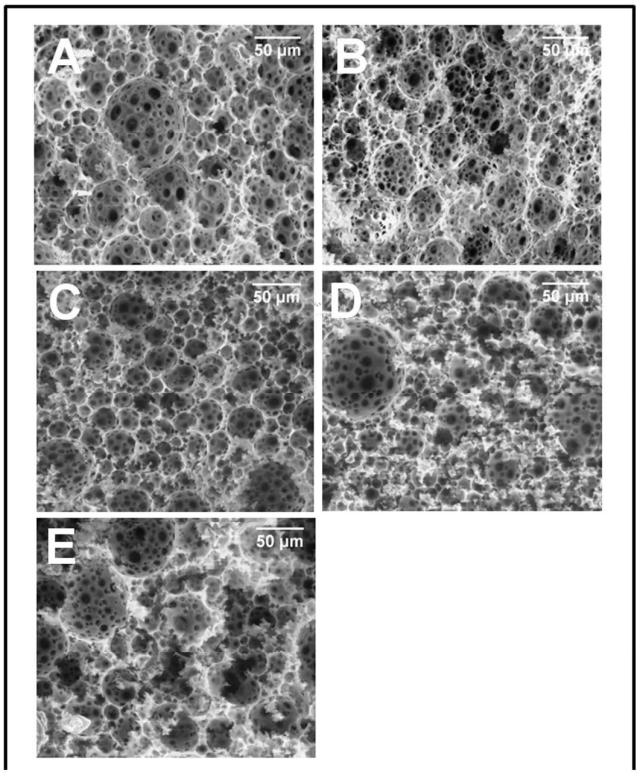

Fig. 3 SEM microscopic images of polyHIPE hydrogels: A) GHG-1, B) GHG-2, C) GHG-3, D)GHG-4 and E) GHG-5.

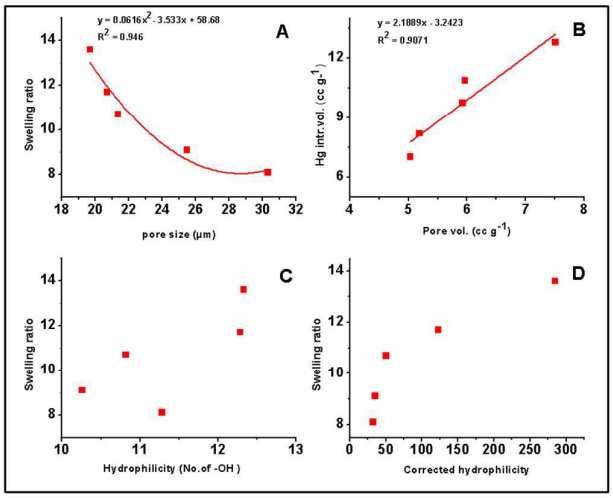

Fig.4 Variation of swelling ratio of polyHIPE hydrogels with A) pore size, C) hydrophilicity, D) corrected hydrophilicity; and B) correlation between Hg intrusion volume and pore volume.

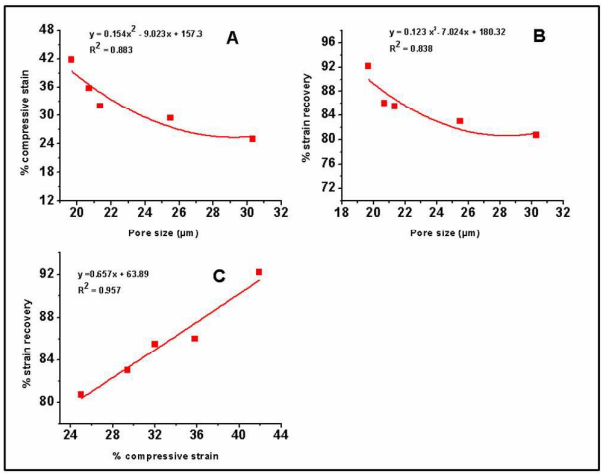

Fig. 5 Variation of mechanical properties of polyHIPE hydrogels with pore size: A) compressive strain, B) strain recovery and C) correlation between compressive strain and strain recovery.

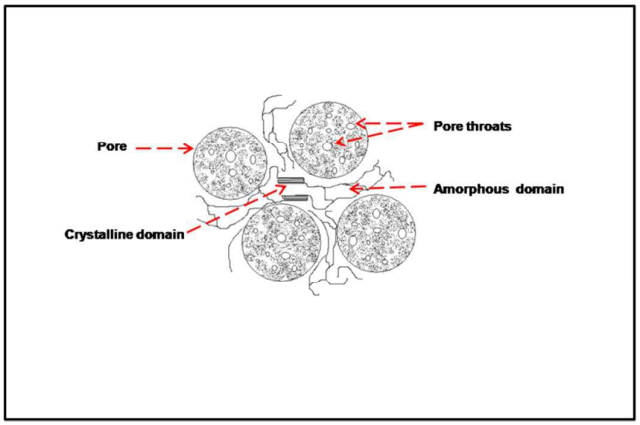

Fig. 7 A schematic amorphous-crystalline model of GMMA-HEMA-GDMA polyHIPE hydrogels (GHG-1to GHG-4); crystallinity decreases from GHG-1 to GHG-4 (not shown).

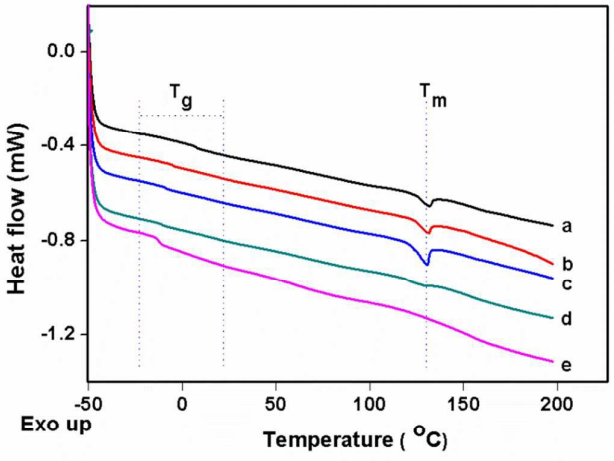

Fig. 6 DSC thermograms of polyHIPE hydrogels: a) GHG-1, b) GHG-2, c) GHG-3, d) GHG-4 and e) GHG-5.

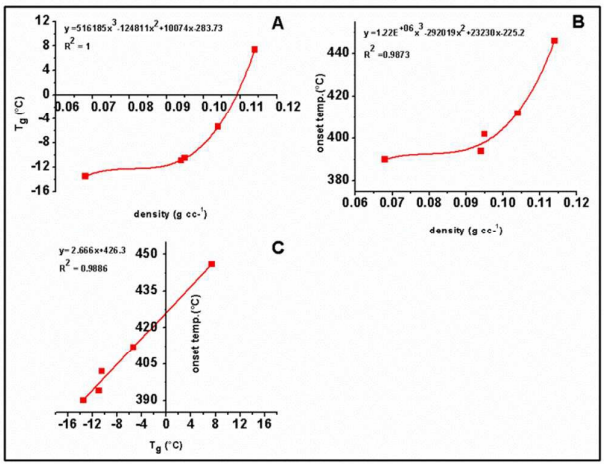

Fig. 8 Variation of glass transition temperature (T_g) and decomposition onset temperature with density A) and B); C) correlation of T_g and decomposition onset temperature.

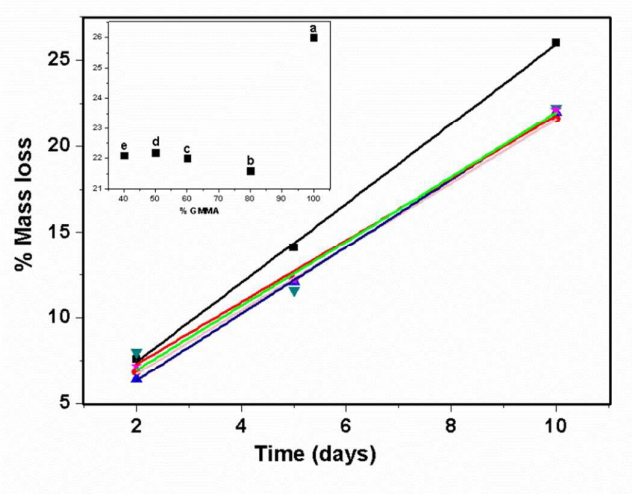

Fig. 9 Degradation of polyHIPE hydrogels in 0.007M NaOH with time at ambient temperature: a) GHG-1, b) GHG-2, c) GHG-3, d) GHG-4 and e) GHG-5; inset: % mass loss vs. % GMMA after 10 days.

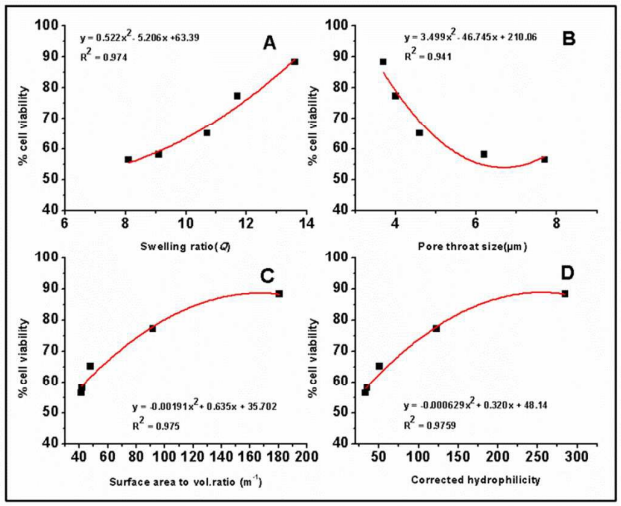

Fig.12 Variation of cell viability with A) swelling ratio, B) pore throat size, C) surface area to volume ratio and D) corrected hydrophilicity.

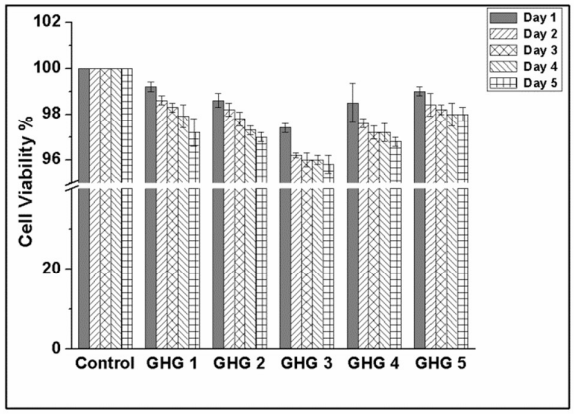

Fig. 10 Cytotoxicity test on NIH3T3 cells in presence of polyHIPE hydrogels by MTT assay.

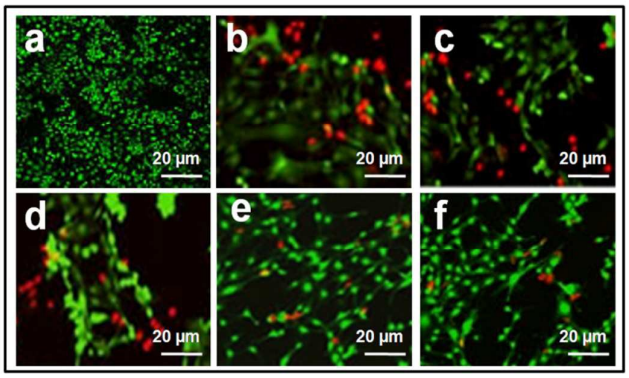

Fig.13 Fluorescence microscopic images of NIH3T3 cells seeded on polyHIPE hydrogels: a) control, b) GHG-1, c) GHG-2, d) GHG-3, e) GHG-4 and f) GHG-5 after 7 days. (It may be noted that the live cells (green) continually increase and the dead cells (red) decrease from GHG-1 to GHG-5, see the text also).

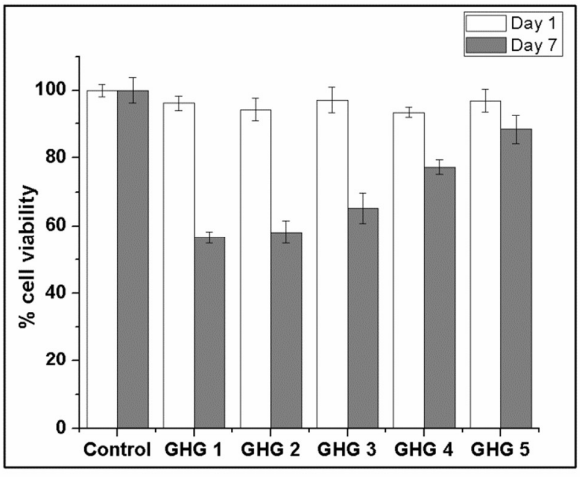

Fig.11 Cell proliferation test on polyHIPE hydrogels relative to TCPS as control by MTT assay.

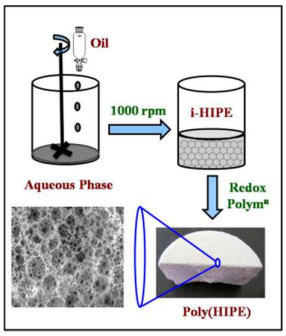

TOC – Synthesis of superporous hydrogels as tissue engineering scaffold via inverse high internal phase emulsion (i-HIPE) polymerization.